

# LOWER BOUND ON $\Gamma(Z \rightarrow \tilde{g}\tilde{g})$ BASED ON UNITARITY<sup>1</sup>

Zumin Luo<sup>2</sup>

*Enrico Fermi Institute and Department of Physics  
University of Chicago, 5640 S. Ellis Avenue, Chicago, IL 60637*

The  $Z$  boson can decay to a pair of light (12–16 GeV) gluinos through loop-mediated processes. In the presence of a light (2–5.5 GeV) bottom squark, the decay width of  $Z \rightarrow \tilde{g}\tilde{g}$  is found to be at least of the order 0.01 MeV based on unitarity of the  $S$ -matrix. Implications of this lower bound are discussed.

PACS Categories: 11.30.Pb, 12.60.Jv, 13.38.Dg, 14.80.Ly

---

<sup>1</sup>Enrico Fermi Institute preprint EFI 03-02  
<sup>2</sup>zuminluo@midway.uchicago.edu

# I INTRODUCTION

A relatively light (12–16 GeV) gluino  $\tilde{g}$ , along with a lighter (2–5.5 GeV) bottom squark  $\tilde{b}$ , has been proposed [1] to explain the excess of the cross section for bottom quark production at hadron colliders. The  $\tilde{b}$  squark is assumed to be a mixture of  $\tilde{b}_L$  and  $\tilde{b}_R$ , the superpartners of  $b_L$  and  $b_R$ . Other supersymmetric (SUSY) particles, except the other sbottom  $\tilde{b}'$  and one of the top squarks, are assumed to be sufficiently heavy. The masses of  $\tilde{b}'$  and the light stop are constrained by the electroweak data to be below 180 GeV and 98 GeV, respectively [2]. We follow the convention in [1] to define

$$\begin{pmatrix} \tilde{b} \\ \tilde{b}' \end{pmatrix} = \begin{pmatrix} \cos \theta_{\tilde{b}} & \sin \theta_{\tilde{b}} \\ -\sin \theta_{\tilde{b}} & \cos \theta_{\tilde{b}} \end{pmatrix} \begin{pmatrix} \tilde{b}_R \\ \tilde{b}_L \end{pmatrix} . \quad (1)$$

The introduction of these new particles gives rise to new interactions in various processes. For example, the total decay width of the  $\Upsilon$  is raised since the decay  $\Upsilon \rightarrow \tilde{b}\tilde{b}^*$  [3] is now permitted; the decay width of the  $Z$  boson is also changed [4, 5]. As a result, the extraction of the strong coupling constant  $\alpha_s$  at these two mass scales will be affected. By contributing to the  $\beta$ -function, these SUSY particles slow down the evolution of  $\alpha_s$  with energy scale [6]. The situation has recently been studied in detail by Chiang *et al.* in [7] and no clear-cut decision can be made in favor of either the Standard Model evolution or the evolution in the light-gluino/light-sbottom scenario. The partial decay width  $\Gamma(Z \rightarrow \tilde{g}\tilde{g})$  remains a key quantity to be determined. A better evaluation of  $\Gamma(Z \rightarrow \tilde{g}\tilde{g})$ , among other things, can improve our understanding of the effect of this scenario on the electroweak measurable at the  $Z$  pole and hence the determination of  $\alpha_s(M_Z)$  in the scenario.

To validate the proposition of these new particles, direct searches for light gluinos and light sbottoms at  $e^-e^+$  colliders will definitely play a key role. An analysis has been presented recently by Berge and Klasen [8] of gluino pair production at linear  $e^-e^+$  colliders. However, they only considered the mass range  $m_{\tilde{g}} \geq 200$  GeV. Production of light gluino pairs was studied, though, by Ref. [9] and its updated version [10]. However, a light sbottom was not included in either of these calculations. Production of light gluinos at  $p\bar{p}$  colliders was considered by Terekhov and Clavelli [11] but without inclusion of the light sbottom either. Therefore, an analysis of light gluino production in the presence of a light sbottom will be very useful for gluino searches.

Previous calculations [10, 12, 13] indicate that the branching ratio of  $Z \rightarrow \tilde{g}\tilde{g}$  falls in the range of  $10^{-5}$  to  $10^{-4}$  for a wide range of MSSM parameters but without the light sbottom  $\tilde{b}$ . This gives a partial width of less than  $\mathcal{O}(1)$  MeV. It is argued in [7] that inclusion of  $\tilde{b}$  should only change the partial width by a very small amount. It is the purpose of this paper to verify this argument and give a reasonable lower bound on  $\Gamma(Z \rightarrow \tilde{g}\tilde{g})$ . A full calculation involves evaluation of triangle Feynman diagrams [9, 10]. Though ultraviolet divergences cancel within a complete isodoublet, one has to remove singularities due to on-shell particles [13]. However, since  $2m_b < M_Z$  and  $2m_{\tilde{b}} < M_Z$ , the Feynman amplitudes have an imaginary part which is finite and can be calculated precisely in an easier way. It is likely that the imaginary parts provide a fairly good estimate of the full amplitudes as long as cancellations

of loop contributions with high internal momenta are implemented. The situation is analogous to the  $K_S$ – $K_L$  mass difference and the decay  $K_L \rightarrow \mu^+ \mu^-$  [14]. In each case the high-momentum components of the loop diagrams are suppressed (here, through the presence of the charmed quark [15]), leaving the low-mass on-shell states ( $\pi\pi$  or  $\gamma\gamma$ , respectively) to provide a good estimate of the matrix element.

The paper is organized as follows: Section II establishes the unitarity relation of the  $\mathcal{M}$  matrix elements; explicit expressions for Dirac and Majorana spinors are given in Section III; amplitudes of the cut diagrams (Fig. 1) are calculated in Section IV and the results are listed in the Appendix; a lower bound on  $\Gamma(Z \rightarrow \tilde{g}\tilde{g})$  is presented in Section V; implications of this lower bounds are discussed in Sections VI and VII; Section VIII summarizes.

## II UNITARITY RELATION

Let us first review the decays  $K_{L,S} \rightarrow l^- l^+$  considered in Ref. [14]. As is the case with  $Z \rightarrow \tilde{g}\tilde{g}$ , both decays are forbidden at the tree level. However, they can occur through a two-photon ( $\gamma\gamma$ ) intermediate state. Other intermediate states such as  $\pi\pi\gamma$  and  $3\pi$  are much less important. As a consequence of the unitarity of the  $S$ -matrix ( $S^\dagger S \equiv (1 + iT)^\dagger (1 + iT) = 1$ ), the  $T$ -matrix element between the initial state  $K_{L,S}$  and the final state  $l^- l^+$  satisfies the following relation

$$\begin{aligned} \text{Im} [\langle l^- l^+ | T | K_{L,S} \rangle] &= \frac{1}{2} [\langle l^- l^+ | T^\dagger T | K_{L,S} \rangle] \\ &= \frac{1}{2} \sum_{\epsilon, \epsilon'} \int \frac{d^3 k}{(2\pi)^3} \frac{d^3 k'}{(2\pi)^3} \frac{1}{2E} \frac{1}{2E'} \langle l^- l^+ | T^\dagger | \gamma(k, \epsilon) \gamma'(k', \epsilon') \rangle \\ &\quad \times \langle \gamma(k, \epsilon) \gamma'(k', \epsilon') | T | K_{L,S} \rangle, \end{aligned} \quad (2)$$

where  $\text{Im}$  denotes the imaginary part and  $|\gamma(k, \epsilon) \gamma'(k', \epsilon')\rangle$  is a real two-photon state with  $k$  and  $k'$ ,  $\epsilon$  and  $\epsilon'$  specifying the 4-momenta and 4-polarizations, respectively. Since the  $T$ -matrix elements can be expressed as the invariant  $\mathcal{M}$  matrix elements multiplied by 4-momentum-conserving  $\delta$ -functions, Eq. (2) becomes

$$\begin{aligned} \text{Im} [\mathcal{M}(K_{L,S} \rightarrow l^- l^+)] &= \frac{1}{2} \sum_{\epsilon, \epsilon'} \int \frac{d^3 k}{(2\pi)^3} \frac{d^3 k'}{(2\pi)^3} \frac{1}{2E} \frac{1}{2E'} \langle \gamma(k, \epsilon) \gamma'(k', \epsilon') | \mathcal{M} | K_{L,S} \rangle \\ &\quad \langle \gamma(k, \epsilon) \gamma'(k', \epsilon') | \mathcal{M} | l^- l^+ \rangle^* (2\pi)^4 \delta^{(4)}(p - k_1 - k_2), \end{aligned} \quad (3)$$

times an overall  $\delta^{(4)}(p - p_1 - p_2)$ , with  $p$ ,  $p_1$  and  $p_2$  being the 4-momenta of  $K_{L,S}$ ,  $l^-$  and  $l^+$ , respectively. It is expected that the real part of the amplitude is roughly of the same order as the imaginary part, so that the actual decay width will exceed the lower bound based on the imaginary part by only a small factor.

Quite similarly, the imaginary part of the invariant matrix element  $\mathcal{M}(Z \rightarrow \tilde{g}\tilde{g})$  can be written as

$$\text{Im} [\mathcal{M}(Z \rightarrow \tilde{g}\tilde{g})] = \frac{1}{2} \sum_f \int d\Pi_f \mathcal{M}(Z \rightarrow f) \mathcal{M}^*(\tilde{g}\tilde{g} \rightarrow f) (2\pi)^4 \delta^{(4)}(p - \sum_{i=1}^{n_f} p_i), \quad (4)$$

where the sum runs over all possible intermediate on-shell states  $f$  and  $d\Pi_f = \prod_{i=1}^{n_f} \frac{d^3 p_i}{(2\pi)^3} \frac{1}{2E_i}$  with  $n_f$  being the numbers of particles in state  $f$  and  $p_i$  being the 3-momenta of the particles. Since  $\tilde{b}$  is the lightest supersymmetric particle in the scenario and all other supersymmetric particles (except  $\tilde{g}$ ) are expected to be heavier than  $M_Z/2$ , we only need to consider the cases where  $f$  is  $b\bar{b}$  and  $\tilde{b}\tilde{b}^*$ .

The integral over the phase space  $\Pi_f$  can be simplified to the integral over the solid angle  $\Omega$ . In the case where  $n_f = 2$ , we have  $\int d\Pi_f (2\pi)^4 \delta^{(4)}(p - \sum_{i=1}^{n_f} p_i) = \frac{1}{32\pi^2} \int d\Omega$ , where  $d\Omega = \sin\theta d\theta d\phi$ . Here  $\theta$  and  $\phi$  are polar angles of  $\mathbf{p}_1$  with respect to the  $z$ -axis.

### III DIRAC AND MAJORANA SPINORS

The uncrossed cut Feynman diagrams that contribute to the imaginary part of the full amplitude are shown in Fig. 1. The crossed diagrams  $\tilde{g}(k_1) \leftrightarrow \tilde{g}(k_2)$  are not shown but should be included in the calculation with an overall minus sign. In the center-of-mass frame of the  $Z$  boson, the 4-momenta of the final gluinos are  $k_1 = (E, \mathbf{k})$  and  $k_2 = (E, -\mathbf{k})$ , where  $E = M_Z/2$  and  $\mathbf{k} = (0, 0, |\mathbf{k}|)$ . Suppose  $\mathbf{k}$  is along the  $z$ -axis and the polarizations of the  $Z$  are quantized along this axis, i.e.,  $\epsilon^\mu = (0, 1, \pm i, 0)/\sqrt{2}$  or  $(0, 0, 0, 1)$ , corresponding to helicities  $\lambda = \pm 1$  or  $0$  respectively. The 4-momenta of the intermediate bottom quarks are  $p_1 = (E, \mathbf{p})$  and  $p_2 = (E, -\mathbf{p})$ , with  $\mathbf{p} = |\mathbf{p}|(\sin\theta \cos\phi, \sin\theta \sin\phi, \cos\theta)$ .

Before evaluating the amplitudes of the diagrams, we first specify the convention we will use and give explicit expressions for the Dirac and Majorana spinors. We adopt the convention of spinors of Peskin and Schroeder [16], in which the metric tensor  $g_{\mu\nu} = \text{Diagonal}(1, -1, -1, -1)$  and

$$\gamma^0 = \begin{pmatrix} 0 & 1 \\ 1 & 0 \end{pmatrix}, \quad \gamma^5 = \begin{pmatrix} -1 & 0 \\ 0 & 1 \end{pmatrix} \quad \text{and} \quad \gamma^i = \begin{pmatrix} 0 & \sigma^i \\ -\sigma^i & 0 \end{pmatrix}, i = 1, 2, 3, \quad (5)$$

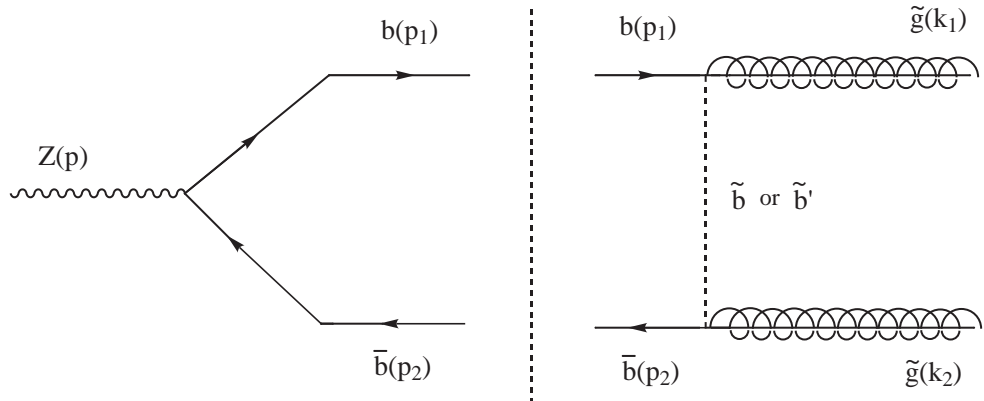
where  $\sigma^i$  are the Pauli matrices. The Dirac spinors in this representation can be written as

$$u^s(p) = \begin{pmatrix} \sqrt{p \cdot \sigma} \xi_p^s \\ \sqrt{p \cdot \bar{\sigma}} \xi_p^s \end{pmatrix}, \quad v^s(p) = \begin{pmatrix} \sqrt{p \cdot \sigma} \eta_p^s \\ -\sqrt{p \cdot \bar{\sigma}} \eta_p^s \end{pmatrix}, \quad (6)$$

where  $\sigma^\mu = (1, \sigma^i)$ ,  $\bar{\sigma}^\mu = (1, -\sigma^i)$ ,  $s$  is the spin index and  $p$  specifies the corresponding 4-momentum. The two-component spinors  $\xi_p^s$  and  $\eta_p^s$  are related via a “spin-flipping” matrix:  $\eta_p^s = -i\sigma^2(\xi_p^s)^*$ . We will use the arrows  $\uparrow$  and  $\downarrow$  to denote spin up and spin down along  $\mathbf{p}$ , respectively. After taking the square roots of the  $2 \times 2$  matrices in Eq. (6), we obtain

$$\begin{aligned} u^\uparrow(p_1) &= \begin{pmatrix} \sqrt{E - |\mathbf{p}|} \xi_1^\uparrow \\ \sqrt{E + |\mathbf{p}|} \xi_1^\uparrow \end{pmatrix} & u^\downarrow(p_1) &= \begin{pmatrix} \sqrt{E + |\mathbf{p}|} \xi_1^\downarrow \\ \sqrt{E - |\mathbf{p}|} \xi_1^\downarrow \end{pmatrix} \\ v^\uparrow(p_2) &= \begin{pmatrix} \sqrt{E - |\mathbf{p}|} \eta_2^\uparrow \\ -\sqrt{E + |\mathbf{p}|} \eta_2^\uparrow \end{pmatrix} & v^\downarrow(p_2) &= \begin{pmatrix} \sqrt{E + |\mathbf{p}|} \eta_2^\downarrow \\ -\sqrt{E - |\mathbf{p}|} \eta_2^\downarrow \end{pmatrix}, \end{aligned} \quad (7)$$

(a)



(b)

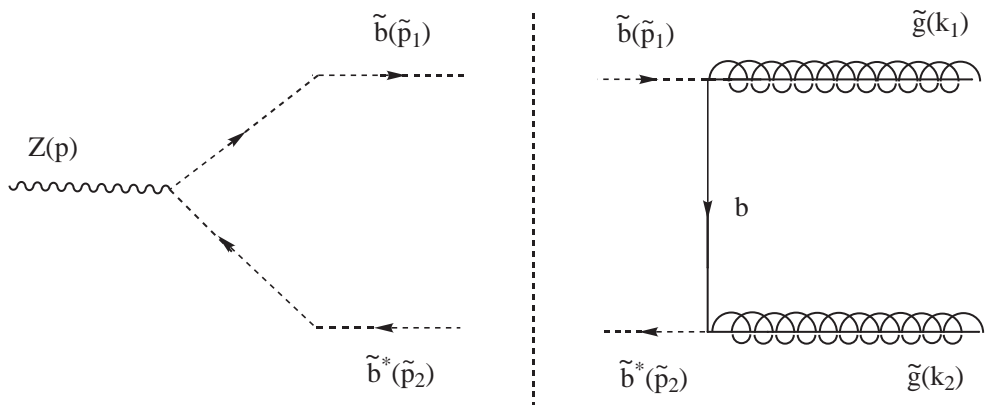


Figure 1: Cut Feynman diagrams for  $Z \rightarrow \tilde{g}\tilde{g}$ : (a)  $Z \rightarrow (b\bar{b})^* \rightarrow \tilde{g}\tilde{g}$ , (b)  $Z \rightarrow (\tilde{b}\tilde{b}^*)^* \rightarrow \tilde{g}\tilde{g}$ . Similar diagrams with  $\tilde{g}(k_1) \leftrightarrow \tilde{g}(k_2)$  are not shown but should be included in the calculation with an overall minus sign.

where

$$\begin{aligned}\xi^\uparrow \equiv \xi_{p_1}^\uparrow &= \begin{pmatrix} \cos \frac{\theta}{2} \\ e^{i\phi} \sin \frac{\theta}{2} \end{pmatrix} & \text{and} & \quad \xi^\downarrow \equiv \xi_{p_1}^\downarrow &= \begin{pmatrix} -e^{-i\phi} \sin \frac{\theta}{2} \\ \cos \frac{\theta}{2} \end{pmatrix} \\ \eta^\uparrow \equiv \eta_{p_2}^\uparrow &= \begin{pmatrix} -\sin \frac{\theta}{2} \\ e^{i\phi} \cos \frac{\theta}{2} \end{pmatrix} & \text{and} & \quad \eta^\downarrow \equiv \eta_{p_2}^\downarrow &= \begin{pmatrix} e^{-i\phi} \cos \frac{\theta}{2} \\ \sin \frac{\theta}{2} \end{pmatrix}\end{aligned}\quad (8)$$

It can be easily verified that  $u(p, s) = C\bar{v}^T(p, s)$  and  $v(p, s) = C\bar{u}^T(p, s)$ , where  $T$  means “transpose” and  $C = i\gamma^0\gamma^2$  is the charge conjugate matrix. The Majorana spinors  $u_{\tilde{g}}$  and  $v_{\tilde{g}}$  also satisfy these relations [17]. Thus we can immediately write

$$\begin{aligned}u_{\tilde{g}}^\uparrow(k_1) &= \begin{pmatrix} \sqrt{E - |\mathbf{k}|} \zeta_+ \\ \sqrt{E + |\mathbf{k}|} \zeta_+ \end{pmatrix} & u_{\tilde{g}}^\downarrow(k_1) &= \begin{pmatrix} \sqrt{E + |\mathbf{k}|} \zeta_- \\ \sqrt{E - |\mathbf{k}|} \zeta_- \end{pmatrix} \\ u_{\tilde{g}}^\uparrow(k_2) &= \begin{pmatrix} \sqrt{E + |\mathbf{k}|} \zeta_+ \\ \sqrt{E - |\mathbf{k}|} \zeta_+ \end{pmatrix} & u_{\tilde{g}}^\downarrow(k_2) &= \begin{pmatrix} -\sqrt{E - |\mathbf{k}|} \zeta_- \\ -\sqrt{E + |\mathbf{k}|} \zeta_- \end{pmatrix} \\ v_{\tilde{g}}^\uparrow(k_1) &= \begin{pmatrix} \sqrt{E + |\mathbf{k}|} \zeta_- \\ -\sqrt{E - |\mathbf{k}|} \zeta_- \end{pmatrix} & v_{\tilde{g}}^\downarrow(k_1) &= \begin{pmatrix} -\sqrt{E - |\mathbf{k}|} \zeta_+ \\ \sqrt{E + |\mathbf{k}|} \zeta_+ \end{pmatrix} \\ v_{\tilde{g}}^\uparrow(k_2) &= \begin{pmatrix} \sqrt{E - |\mathbf{k}|} \zeta_- \\ -\sqrt{E + |\mathbf{k}|} \zeta_- \end{pmatrix} & v_{\tilde{g}}^\downarrow(k_2) &= \begin{pmatrix} \sqrt{E + |\mathbf{k}|} \zeta_+ \\ -\sqrt{E - |\mathbf{k}|} \zeta_+ \end{pmatrix},\end{aligned}\quad (9)$$

with  $\zeta_+ = \begin{pmatrix} 1 \\ 0 \end{pmatrix}$  and  $\zeta_- = \begin{pmatrix} 0 \\ 1 \end{pmatrix}$ . Here the arrows  $\uparrow$  and  $\downarrow$  denote spin up and spin down along  $\mathbf{k}$  (i.e., the  $z$ -axis), respectively. The Feynman rules for the Majorana fields are given in a representation independent way in [17].

## IV AMPLITUDES OF THE CUT DIAGRAMS

The  $\mathcal{M}$  matrix element for  $Z \rightarrow b\bar{b}$  is

$$\mathcal{M}(Z \rightarrow b\bar{b}) = -\frac{g_W}{2 \cos \theta_W} \bar{u}(p_1) \not{e}(p) (g_L P_L + g_R P_R) v(p_2) \delta^{ij}, \quad (10)$$

where  $\not{e} \equiv \epsilon \cdot \gamma$ ,  $g_L = g_V + g_A = \frac{2}{3} \sin^2 \theta_W - 1$ ,  $g_R = g_V - g_A = \frac{2}{3} \sin^2 \theta_W$ ,  $P_L = \frac{1-\gamma^5}{2}$ ,  $P_R = \frac{1+\gamma^5}{2}$ ,  $\delta^{ij}$  is a Kronecker delta in the quark color indices and  $p = p_1 + p_2$  is the 4-momentum of the  $Z$ . Using the notations in the previous section, we have

$$\begin{aligned}\mathcal{M}(Z \rightarrow b^\uparrow \bar{b}^\uparrow) &= (0, i \sin \phi + \cos \phi \cos \theta, -i \cos \phi + \sin \phi \cos \theta, -\sin \theta) \cdot \epsilon(p) \\ &\quad \times \frac{g_W}{2 \cos \theta_W} [(E - |\mathbf{p}|) g_L + (E + |\mathbf{p}|) g_R] \delta^{ij} \\ \mathcal{M}(Z \rightarrow b^\downarrow \bar{b}^\downarrow) &= (0, -i \sin \phi + \cos \phi \cos \theta, i \cos \phi + \sin \phi \cos \theta, -\sin \theta) \cdot \epsilon(p) \\ &\quad \times \frac{g_W}{2 \cos \theta_W} [(E + |\mathbf{p}|) g_L + (E - |\mathbf{p}|) g_R] \delta^{ij}\end{aligned}$$

$$\begin{aligned}
\mathcal{M}(Z \rightarrow b^\dagger \bar{b}^\dagger) &= \frac{g_W m_b}{2 \cos \theta_W} e^{-i\phi} [g_L(-1, \sin \theta \cos \phi, \sin \theta \sin \phi, \cos \theta) \\
&\quad + g_R(1, \sin \theta \cos \phi, \sin \theta \sin \phi, \cos \theta)] \cdot \epsilon(p) \delta^{ij} \\
\mathcal{M}(Z \rightarrow b^\dagger \bar{b}^\dagger) &= -\frac{g_W m_b}{2 \cos \theta_W} e^{i\phi} [g_L(1, \sin \theta \cos \phi, \sin \theta \sin \phi, \cos \theta) \\
&\quad + g_R(-1, \sin \theta \cos \phi, \sin \theta \sin \phi, \cos \theta)] \cdot \epsilon(p) \delta^{ij}
\end{aligned}$$

For  $\sin^2 \theta_W = 0.2311$  and without top quark corrections, the partial decay width for  $Z$  to decay into massless  $b\bar{b}$  is then  $\frac{G_F M_Z^3}{4\sqrt{2}\pi} (g_L^2 + g_R^2) = 368$  MeV. Now we consider  $b\bar{b} \rightarrow \tilde{g}\tilde{g}$  via exchange of a  $\tilde{b}$  or  $\tilde{b}'$ , the matrix element for which is denoted  $\mathcal{M}(b\bar{b} \rightarrow \tilde{g}\tilde{g})$  or  $\mathcal{M}'(b\bar{b} \rightarrow \tilde{g}\tilde{g})$ , respectively. We have  $\mathcal{M}(b\bar{b} \rightarrow \tilde{g}\tilde{g}) = \mathcal{M}^{(1)}(b\bar{b} \rightarrow \tilde{g}\tilde{g}) + \mathcal{M}^{(2)}(b\bar{b} \rightarrow \tilde{g}\tilde{g})$ , with

$$\mathcal{M}^{(1)}(b\bar{b} \rightarrow \tilde{g}\tilde{g}) = -2g_s^2 \frac{(t^b t^a)_{ji}}{(p_1 - k_1)^2 - m_{\tilde{b}}^2} \bar{u}_{\tilde{g}}(k_1) (P_L \sin \theta_{\tilde{b}} - P_R \cos \theta_{\tilde{b}}) u(p_1) \\
\bar{v}(p_2) (P_R \sin \theta_{\tilde{b}} - P_L \cos \theta_{\tilde{b}}) v_{\tilde{g}}(k_2), \quad (11)$$

$$\mathcal{M}^{(2)}(b\bar{b} \rightarrow \tilde{g}\tilde{g}) = -2g_s^2 \frac{(t^a t^b)_{ji}}{(p_1 - k_2)^2 - m_{\tilde{b}}^2} v_{\tilde{g}}^T(k_2) C^{-1} (P_L \sin \theta_{\tilde{b}} - P_R \cos \theta_{\tilde{b}}) u(p_1) \\
\bar{v}(p_2) (P_R \sin \theta_{\tilde{b}} - P_L \cos \theta_{\tilde{b}}) C \bar{u}_{\tilde{g}}^T(k_1), \quad (12)$$

where the superscript (1) denotes the uncrossed diagram and (2) the crossed diagram;  $a, b$  and  $i, j$  are the color indices of the gluinos and the quarks, respectively;  $t^a$  are the fundamental representation matrices of  $SU(3)$ . Since  $v_{\tilde{g}}^T(k_2) C^{-1} = -\bar{u}_{\tilde{g}}(k_2)$  and  $C \bar{u}_{\tilde{g}}^T(k_1) = v_{\tilde{g}}(k_1)$ , Eq. (12) can alternatively be obtained from Eq. (11) by interchanging  $k_1$  and  $k_2$  and adding an overall minus sign. The helicities of the final gluinos are determined by  $\lambda$ , the initial helicity of the  $Z$ . For  $\lambda = 1$ , both gluinos have spin up in the  $z$ -direction, while for  $\lambda = -1$ , both have spin down in the  $z$ -direction. For  $\lambda = 0$ , one of them has spin up and the other has spin down in the  $z$ -direction. One expects  $|\text{Im} \mathcal{M}(Z^\dagger \rightarrow \tilde{g}^\dagger \tilde{g}^\dagger)| = |\text{Im} \mathcal{M}(Z^\dagger \rightarrow \tilde{g}^\dagger \tilde{g}^\dagger)|$ , because the two processes are related by mirror symmetry. One also expects  $\text{Im} \mathcal{M}(Z^{(0)} \rightarrow \tilde{g}^\dagger \tilde{g}^\dagger) = 0$ , because these final gluinos have the same helicities and should therefore be excluded by the Pauli principle. Therefore only the  $\mathcal{M}$  matrix elements for  $\lambda = 1$  are listed in the Appendix. The matrix element  $\mathcal{M}'(b\bar{b} \rightarrow \tilde{g}\tilde{g})$  can be obtained from  $\mathcal{M}(b\bar{b} \rightarrow \tilde{g}\tilde{g})$  by replacing  $m_{\tilde{b}}$ ,  $\sin \theta_{\tilde{b}}$  and  $\cos \theta_{\tilde{b}}$  with  $m_{\tilde{b}'}$ ,  $\cos \theta_{\tilde{b}}$  and  $-\sin \theta_{\tilde{b}}$ , respectively.

Now we consider the diagram in Fig. 1 (b) and a similar diagram with  $\tilde{g}(k_1) \leftrightarrow \tilde{g}(k_2)$ , where the intermediate state is a pair of scalar quarks ( $\tilde{b}$  and  $\tilde{b}^*$ ). The tree-level  $Z\tilde{b}\tilde{b}^*$  coupling is proportional to  $g_L \sin^2 \theta_{\tilde{b}} + g_R \cos^2 \theta_{\tilde{b}}$ , so a mixing angle of  $\theta_{\tilde{b}} = \arcsin \sqrt{2 \sin^2 \theta_W / 3} \simeq 23^\circ$  or  $157^\circ$  will make it vanish. A weak  $Z\tilde{b}\tilde{b}^*$  coupling is assumed [1] to satisfy the tight constraints imposed by precision measurements at the  $Z$  peak. Consequently the contribution of the  $\tilde{b}\tilde{b}^*$  intermediate state to  $\text{Im} \mathcal{M}(Z \rightarrow \tilde{g}\tilde{g})$  will also be small. However, to see how the two types of diagrams shown in Fig. 1 interfere with each other, here we take  $\theta_{\tilde{b}}$  to be a free parameter. For the first part of the cut diagram (Fig. 1 (b)), we have

$$\mathcal{M}(Z \rightarrow \tilde{b}\tilde{b}^*) = -\frac{g_W}{2 \cos \theta_W} [g_L \sin^2 \theta_{\tilde{b}} + g_R \cos^2 \theta_{\tilde{b}}] (\tilde{p}_1 - \tilde{p}_2)^\mu \epsilon_\mu(p) \delta^{ij}, \quad (13)$$

where  $i$  and  $j$  are the squark color indices. For the other part of the diagram,

$$\begin{aligned} \mathcal{M}^{(1)}(\tilde{b}\tilde{b}^* \rightarrow \tilde{g}\tilde{g}) &= 2g_s^2 \frac{(t^b t^a)_{ji}}{(\tilde{p}_1 - k_1)^2 - m_b^2} v_{\tilde{g}}^T(k_2) C^{-1} [P_L \sin \theta_{\tilde{b}} - P_R \cos \theta_{\tilde{b}}] \\ &\quad (\tilde{p}_1 - \not{k}_1 + m_b) [P_R \sin \theta_{\tilde{b}} - P_L \cos \theta_{\tilde{b}}] C \bar{u}_{\tilde{g}}^T(k_1) \end{aligned} \quad (14)$$

$$\begin{aligned} \mathcal{M}^{(2)}(\tilde{b}\tilde{b}^* \rightarrow \tilde{g}\tilde{g}) &= 2g_s^2 \frac{(t^a t^b)_{ji}}{(\tilde{p}_1 - k_2)^2 - m_b^2} \bar{u}_{\tilde{g}}(k_1) [P_L \sin \theta_{\tilde{b}} - P_R \cos \theta_{\tilde{b}}] \\ &\quad (\tilde{p}_1 - \not{k}_2 + m_b) [P_R \sin \theta_{\tilde{b}} - P_L \cos \theta_{\tilde{b}}] v_{\tilde{g}}(k_2), \end{aligned} \quad (15)$$

where (1) denotes the uncrossed diagram and (2) the crossed diagram. The relevant matrix elements for  $\lambda = 1$  are presented in the Appendix.

## V LOWER BOUND ON $\Gamma(Z \rightarrow \tilde{g}\tilde{g})$

Now we are ready to put things together and obtain a lower bound on  $\Gamma(Z \rightarrow \tilde{g}\tilde{g})$ . First we consider an extreme case with  $m_b = m_{\tilde{b}} = m_{\tilde{g}} = 0$  and  $m_{\tilde{b}'} = \infty$ . In this limit, the product  $\mathcal{M}(Z \rightarrow f)\mathcal{M}(f \rightarrow \tilde{g}\tilde{g})$  has an angular dependence of either  $(1 + \cos \theta)$  or  $(1 - \cos \theta)$ . However, the  $\cos \theta$  term does not contribute to the imaginary part of the full amplitude, because integrating it over the solid angle  $\Omega$  gives zero. Note that  $\text{tr}(t^a t^b) = \text{tr}(t^b t^a) = \delta^{ab}/2$ . The only nonvanishing amplitudes are then

$$\begin{aligned} \mathcal{M}(Z^\uparrow \rightarrow b\bar{b})\mathcal{M}(b\bar{b} \rightarrow \tilde{g}^\uparrow \tilde{g}^\uparrow) &= -\mathcal{M}(Z^\downarrow \rightarrow b\bar{b})\mathcal{M}(b\bar{b} \rightarrow \tilde{g}^\downarrow \tilde{g}^\downarrow) \\ &= \frac{\delta^{ab}}{2} \frac{M_Z g_W g_s^2}{\sqrt{2} \cos \theta_W} g_- \\ \mathcal{M}(Z^\uparrow \rightarrow \tilde{b}\tilde{b}^*)\mathcal{M}(\tilde{b}\tilde{b}^* \rightarrow \tilde{g}^\uparrow \tilde{g}^\uparrow) &= -\mathcal{M}(Z^\downarrow \rightarrow \tilde{b}\tilde{b}^*)\mathcal{M}(\tilde{b}\tilde{b}^* \rightarrow \tilde{g}^\downarrow \tilde{g}^\downarrow) \\ &= \frac{\delta^{ab}}{2} \frac{M_Z g_W g_s^2}{\sqrt{2} \cos \theta_W} g_+ \cos 2\theta_{\tilde{b}} \end{aligned}$$

where we have summed over the four helicity states of  $b\bar{b}$ ,  $g_\pm = g_L \sin^2 \theta_{\tilde{b}} \pm g_R \cos^2 \theta_{\tilde{b}}$ . From the above two equations we can see that the two types of diagrams in Fig. 1 interfere destructively if  $\tilde{b}$  is more left-handed ( $45^\circ < \theta_{\tilde{b}} < 135^\circ$ ) or dominantly right-handed ( $\theta_{\tilde{b}} < 23^\circ$  or  $\theta_{\tilde{b}} > 157^\circ$ ); the contribution of diagram (b) remains negligible in the neighborhood of the decoupling angle ( $23^\circ$  or  $157^\circ$ ). The imaginary parts of the amplitudes are

$$\begin{aligned} \text{Im}\mathcal{M}(Z^\uparrow \rightarrow \tilde{g}^\uparrow \tilde{g}^\uparrow) &= -\text{Im}\mathcal{M}(Z^\downarrow \rightarrow \tilde{g}^\downarrow \tilde{g}^\downarrow) \\ &= \frac{\delta^{ab}}{16} \frac{M_Z g_W g_s^2}{\sqrt{2} \cos \theta_W} (g_L - g_R) \sin^2 \theta_{\tilde{b}} \cos^2 \theta_{\tilde{b}} \end{aligned} \quad (16)$$

This relation (16) also holds when all the particles have a finite mass. The final result in the limit  $m_b = m_{\tilde{b}} = m_{\tilde{g}} = 0$  and  $m_{\tilde{b}'} = \infty$  can be expressed as a ratio

$$\begin{aligned} \frac{\Gamma(Z \rightarrow \tilde{g}\tilde{g})}{\Gamma(Z \rightarrow b\bar{b})} &\geq \frac{1}{2} \frac{\left| \text{Im}\mathcal{M}(Z^\uparrow \rightarrow \tilde{g}^\uparrow \tilde{g}^\uparrow) \right|^2 + \left| \text{Im}\mathcal{M}(Z^\downarrow \rightarrow \tilde{g}^\downarrow \tilde{g}^\downarrow) \right|^2}{\left| \text{Im}\mathcal{M}(Z^\uparrow \rightarrow b\bar{b}^\uparrow) \right|^2 + \left| \text{Im}\mathcal{M}(Z^\downarrow \rightarrow b\bar{b}^\downarrow) \right|^2} \\ &= \frac{\alpha_s^2}{6} \frac{(g_L - g_R)^2 \sin^4 \theta_{\tilde{b}} \cos^4 \theta_{\tilde{b}}}{g_L^2 + g_R^2} \end{aligned} \quad (17)$$

The factor of  $1/2$  comes in because the final gluinos are identical. Taking  $\Gamma(Z \rightarrow b\bar{b}) = 375.9$  MeV [18], we plot the lower bound on the decay width  $\Gamma(Z \rightarrow \tilde{g}\tilde{g})$  as a function of the sbottom mixing angle  $\theta_{\tilde{b}}$  in Fig. 2. When all the masses are finite, we can no longer ignore the  $\cos \theta$  terms, because the denominators of the propagators are no longer of the form  $\sim (1 \pm \cos \theta)$ , which previously cancelled with the same factors in the numerators of the amplitudes and gave only linear terms in  $\cos \theta$ . However, it is still not hard to perform the integration over the angles. Define

$$\begin{aligned} I_{\pm}(x, y, z) &= \frac{1}{2} \int_0^{\pi} \frac{(1 \pm \cos \theta)^2}{x^2 + y^2 + z^2 + 2xy \cos \theta} \sin \theta d\theta \\ I_0(x, y, z) &= \int_0^{\pi} \frac{\sin^2 \theta}{x^2 + y^2 + z^2 + 2xy \cos \theta} \sin \theta d\theta \quad , \end{aligned}$$

and let  $c_{\pm} = I_{\pm}(v_b, v_{\tilde{g}}, r_{\tilde{b}})$ ,  $c'_{\pm} = I_{\pm}(v_b, v_{\tilde{g}}, r_{\tilde{b}'})$ ,  $c_0 = I_0(v_b, v_{\tilde{g}}, r_{\tilde{b}})$ ,  $c'_0 = I_0(v_b, v_{\tilde{g}}, r_{\tilde{b}'})$ ,  $\tilde{c}_0 = I_0(v_{\tilde{b}}, v_{\tilde{g}}, r_b)$ , where  $r_b = 2m_b/M_Z$ ,  $v_b = \sqrt{1 - r_b^2}$  is the “velocity” of an on-shell  $b$  quark;  $r_{\tilde{b}}$ ,  $r_{\tilde{b}'}$ ,  $r_{\tilde{g}}$  and  $v_{\tilde{g}}$  are defined in a similar way. The *exact* final result can then be written as

$$\Gamma(Z \rightarrow \tilde{g}\tilde{g}) \geq \frac{G_F M_Z^3 \alpha_s^2}{96\sqrt{2}\pi} [c_+(v_b + v_{\tilde{g}})g_- + \tilde{c}_0 v_{\tilde{b}}^2 v_{\tilde{g}} g_+ \cos 2\theta_{\tilde{b}} + O(m)]^2 v_{\tilde{g}} \quad , \quad (18)$$

where  $O(m)$  is the sum of the terms that approach zero when  $m_b$ ,  $m_{\tilde{b}}$  and  $m_{\tilde{g}}$  go to zero. We have  $O(m) = c_1 g_V \cos 2\theta_{\tilde{b}} + c_2 g_A \sin 2\theta_{\tilde{b}} - c_3 g_A$ , with

$$\begin{aligned} c_1 &= (c_- - c'_-)(v_b - v_{\tilde{g}}) + (c_0 - c'_0)r_b^2 v_{\tilde{g}} \\ c_2 &= (c_- - c'_-)r_b r_{\tilde{g}} v_b \\ c_3 &= (c_- + c'_-)(v_b - v_{\tilde{g}}) + (c_+ + c'_+)r_b^2 v_{\tilde{g}} \quad . \end{aligned}$$

The lower bound is plotted in Fig. 2 as a function of  $\theta_{\tilde{b}}$  for a specific set of values for the masses:  $m_b = 4.1$  GeV,  $m_{\tilde{b}} = 4.5$  GeV,  $m_{\tilde{b}'} = 170$  GeV,  $m_{\tilde{g}} = 15$  GeV. The shape of the curve is changed significantly by the masses, especially in the large  $\theta_{\tilde{b}}$  range. This is because a right-handed  $b$  quark couples only to a left-handed  $\tilde{g}$  (and vice versa) in the massless limit while they are chirally mixed if massive. The contribution from a finite  $m_{\tilde{b}'} (\leq 180$  GeV) is less than 5% for most  $\theta_{\tilde{b}}$  (except those around which the lower bound vanishes). The lower bound is about 0.019 MeV near  $\theta_{\tilde{b}} = 23^\circ$  and 0.007 MeV near  $\theta_{\tilde{b}} = 157^\circ$ ; the largest lower bound is 0.064 MeV attained around  $\theta_{\tilde{b}} = 43^\circ$ . We expect the full width to be of this order of magnitude. This can be seen from comparison with the decay  $Z \rightarrow q\bar{q}g^* \rightarrow q\bar{q}\tilde{g}\tilde{g}$  [19]. Both decay widths are  $\sim \alpha\alpha_s^2$  and the phase spaces are similar if  $q$  is a light quark. However,  $Z \rightarrow q\bar{q}g^* \rightarrow q\bar{q}\tilde{g}\tilde{g}$  is mainly a tree process, while  $Z \rightarrow \tilde{g}\tilde{g}$  can only occur through loop processes. The decay width  $\Gamma(Z \rightarrow q\bar{q}g^* \rightarrow q\bar{q}\tilde{g}\tilde{g})$  is calculated in a model-independent way to be  $(0.20 - 0.74)$  MeV [19] for  $m_{\tilde{g}} = 12 - 16$  GeV. (A recent analysis shows that  $\Gamma(Z \rightarrow b\bar{b}\tilde{g}\tilde{g})$  can be enhanced by 1% – 26% due to additional “sbottom splitting” diagrams [20]. This will raise  $\Gamma(Z \rightarrow q\bar{q}\tilde{g}\tilde{g})$  by 0.01 – 0.23 MeV).  $\Gamma(Z \rightarrow \tilde{g}\tilde{g})$  is expected to be less. A very conservative estimate of the upper bound is taken to be 1 MeV [7].

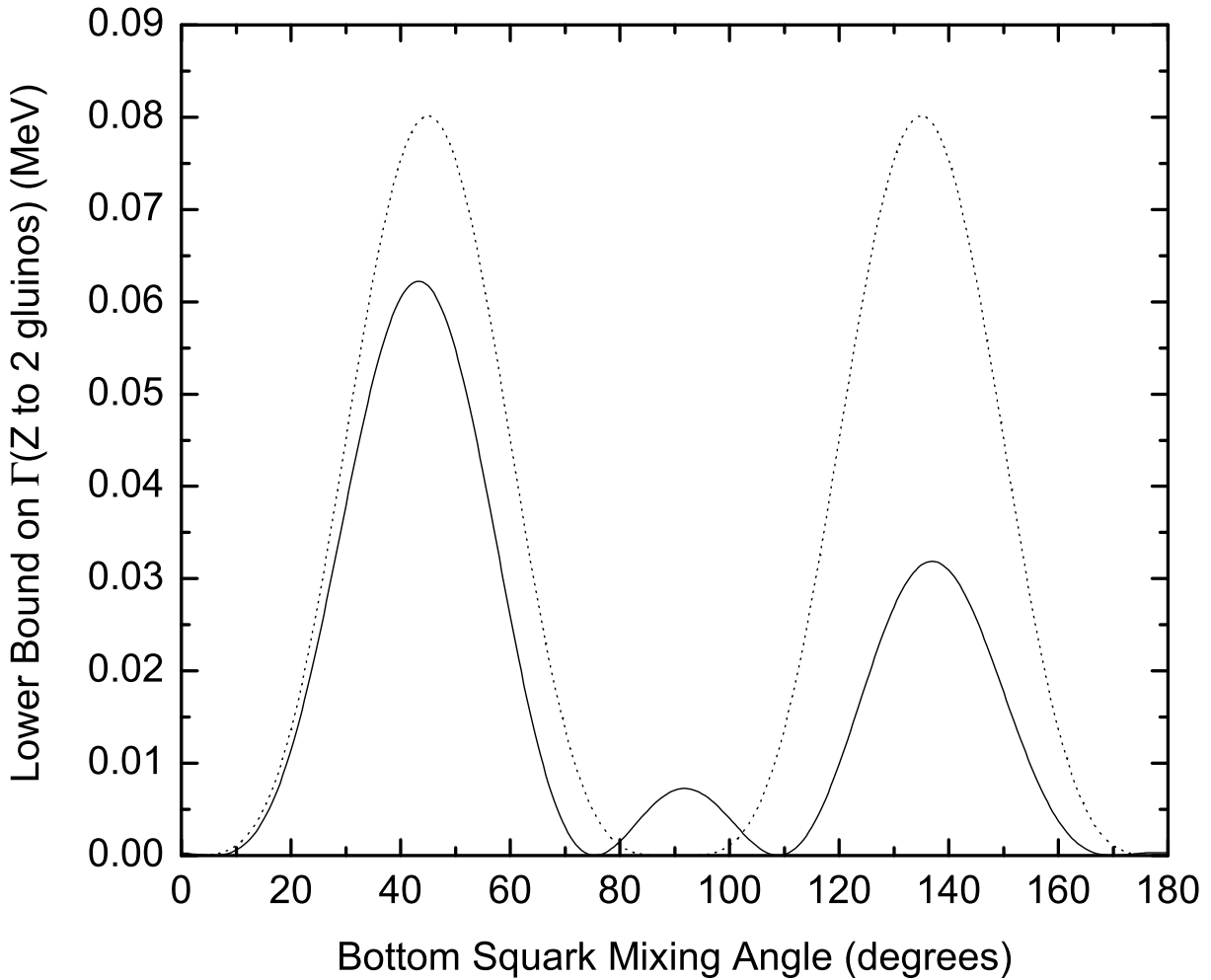


Figure 2: Lower bound on  $\Gamma(Z \rightarrow \tilde{g}\tilde{g})$  as a function of the sbottom mixing angle  $\theta_{\tilde{b}}$ .  
 Solid curve:  $m_b = 4.1$  GeV,  $m_{\tilde{b}} = 4.5$  GeV,  $m_{\tilde{g}} = 15$  GeV,  $m_{\tilde{b}\tilde{b}'} = 170$  GeV; Dotted curve:  $m_b = m_{\tilde{b}} = m_{\tilde{g}} = 0$  and  $m_{\tilde{b}\tilde{b}'} = \infty$ .

## VI IMPLICATIONS FOR GLUINO SEARCHES IN $Z$ DECAYS

Aside from  $Z \rightarrow \tilde{g}\tilde{g}$  and  $Z \rightarrow q\bar{q}g^* \rightarrow q\bar{q}\tilde{g}\tilde{g}$  in which gluinos are produced in pairs, there exist two other gluino-producing  $Z$  decays,  $Z \rightarrow b\bar{b}^* \rightarrow b\tilde{b}^*\tilde{g}$  and  $Z \rightarrow \bar{b}b^* \rightarrow \bar{b}\tilde{b}\tilde{g}$ . These two processes are  $\sim \alpha\alpha_s$  at the tree level and have a combined decay width of 2.5 – 8.0 MeV [21] depending on the sign of  $\sin 2\theta_{\tilde{b}}$ . The new SUSY particles do not always contribute positively to the  $Z$  width, however. Cao *et al.* [5] and S.w. Baek [22] showed that the decay width  $\Gamma(Z \rightarrow b\bar{b})$  can be reduced by as much as 7.8 MeV. By fine-tuning the parameters in the light gluino and light sbottom scenario, all the electroweak measurables ( $\Gamma_Z$ ,  $\Gamma_{\text{had}}(Z)$ ,  $R_b$ ,  $R_c$ ) at the  $Z$  pole can be still within the  $1\sigma$  bounds of the experimental values. Thus, existence of the new particles can only be verified through direct searches for gluinos or sbottoms. The light sbottom is assumed to be long-lived at the collider scale or to decay promptly to light hadrons in this scenario. In either case, it forms a hadronic jet within the detector due to its color charge.  $\tilde{g}$  decays exclusively to  $b\bar{b}^*$  or  $\bar{b}b$  and becomes two hadronic jets. The smallness of the lower bound on  $\Gamma(Z \rightarrow \tilde{g}\tilde{g})$  implies the insignificance of  $Z \rightarrow \tilde{g}\tilde{g}$  in gluino searches. Searches for signals of  $Z \rightarrow q\bar{q}\tilde{g}\tilde{g}$  and  $Z \rightarrow b\bar{b}^*\tilde{g} + \bar{b}\tilde{b}\tilde{g}$  will be expected to play a pivotal role.

## VII IMPLICATIONS FOR RUNNING OF $\alpha_s$

Both the light gluino ( $\tilde{g}$ ) and the light sbottom ( $\tilde{b}$ ) can change the  $\beta$ -function that governs the energy-scale dependence (“running”) of the strong coupling constant  $\alpha_s$ . At two-loop level,  $\alpha_s(M_Z)$  can be raised by  $0.014 \pm 0.001$  [7] with respect to its standard model value if extrapolated from the mass scale  $m_b$ . A natural question arises: are values of  $\alpha_s(M_Z)$  determined from measurements at different energy scales still in accordance in the presence of  $\tilde{g}$  and  $\tilde{b}$ ? To answer this question, the effects of the new SUSY particles on measurements at different scales must be analyzed. For example, the hadronic width of the  $Z$  is changed in two ways: 1) the interference of the standard model diagrams and the diagrams with the SUSY particles in loops will reduce the partial width of  $Z \rightarrow b\bar{b}$ ; 2) the existence of the new decay channels  $Z \rightarrow \tilde{b}\tilde{b}$ ,  $Z \rightarrow \tilde{g}\tilde{g}$ ,  $Z \rightarrow q\bar{q}\tilde{g}\tilde{g}$  and  $Z \rightarrow b\bar{b}^*\tilde{g}/\bar{b}\tilde{b}\tilde{g}$  will raise the hadronic width. The squark mixing angle  $\theta_{\tilde{b}}$  is constrained by the first channel to be near  $23^\circ$  or  $157^\circ$ . The lower bound on the decay width of  $Z \rightarrow \tilde{g}\tilde{g}$  is only of the order 0.01 MeV at either of these two angles (Fig. 2). Thus both channels combined will change the predicted hadronic width of the  $Z$  by a negligible amount if this lower bound provides a good estimate of the actual width for  $Z \rightarrow \tilde{g}\tilde{g}$ . Actually, even if the actual width is about 1 MeV, its effect is still small compared to that of the decrease in  $\Gamma(Z \rightarrow b\bar{b})$  and the increase in  $\Gamma_{\text{had}}(Z)$  due to  $Z \rightarrow q\bar{q}\tilde{g}\tilde{g}$  and  $Z \rightarrow b\bar{b}^*\tilde{g}/\bar{b}\tilde{b}\tilde{g}$ . A better determination of  $\Gamma(Z \rightarrow b\bar{b})$ ,  $\Gamma(Z \rightarrow q\bar{q}\tilde{g}\tilde{g})$  and  $\Gamma(Z \rightarrow b\bar{b}^*\tilde{g}/\bar{b}\tilde{b}\tilde{g})$ , or a more precise measurement of  $R_b$  (which will constrain the value of  $\Gamma(Z \rightarrow b\bar{b})$  more tightly), is needed for a clear-cut decision in favor of either the Standard Model or the light gluino/light sbottom scenario.

## VIII SUMMARY

Instead of calculating the full decay width  $\Gamma(Z \rightarrow \tilde{g}\tilde{g})$  which depends on many other unknown parameters (e.g.,  $m_{\tilde{t}}$ ,  $m_{\tilde{b}}$ ,  $\theta_{\tilde{t}}$ , etc), we have obtained its lower bound as the function of a single parameter  $\theta_{\tilde{b}}$ . The lower bound is of the order 0.01 MeV around  $\theta_{\tilde{b}} = 23^\circ$  or  $157^\circ$ , the decoupling angles for  $Z\tilde{b}\tilde{b}^*$ . This lower bound is valid as long as all other SUSY particles are heavy. We expect the full width to be not far from this lower bound. Compared with other decay processes like  $\Gamma(Z \rightarrow q\bar{q}\tilde{g}\tilde{g})$  and  $\Gamma(Z \rightarrow b\tilde{b}^*\tilde{g}/\bar{b}\tilde{g})$ ,  $Z \rightarrow \tilde{g}\tilde{g}$  will only play a moderate role in searches for gluinos and analysis of effects of the SUSY scenario on  $\alpha_s(M_Z)$ .

## ACKNOWLEDGMENTS

I would like to thank Jonathan L. Rosner and Cheng-Wei Chiang for very useful discussions and suggestions. This work was supported in part by the U. S. Department of Energy through Grant Nos. DE-FG02-90ER-40560.

## APPENDIX: RELEVANT MATRIX ELEMENTS

We define

$$\begin{aligned}
A^{(1)} &= -2g_s^2 \frac{(t^b t^a)_{ji}}{(p_1 - k_1)^2 - m_{\tilde{b}}^2} \\
A^{(2)} &= -2g_s^2 \frac{(t^a t^b)_{ji}}{(p_1 - k_2)^2 - m_{\tilde{b}}^2} \\
\tilde{A}^{(1)} &= -2g_s^2 \frac{(t^b t^a)_{ji}}{(\tilde{p}_1 - k_1)^2 - m_{\tilde{b}}^2} \\
\tilde{A}^{(2)} &= -2g_s^2 \frac{(t^a t^b)_{ji}}{(\tilde{p}_1 - k_2)^2 - m_{\tilde{b}}^2} \\
B_{\pm\pm} &= \sqrt{(E \pm |\mathbf{k}|)(E \pm |\mathbf{p}|)} \\
\tilde{B}_{\pm\pm} &= \sqrt{(E \pm |\mathbf{k}|)(E \pm |\mathbf{k}|)} \\
S_{\tilde{b}} &= \sin \theta_{\tilde{b}} \\
C_{\tilde{b}} &= \cos \theta_{\tilde{b}}
\end{aligned}$$


---

$\mathcal{M}$  matrix elements for  $Z^\uparrow \rightarrow b\bar{b} \rightarrow \tilde{g}^\uparrow \tilde{g}^\uparrow$ :

$$\begin{aligned}
\mathcal{M}(Z^\uparrow \rightarrow b^\uparrow \bar{b}^\uparrow) &= -\frac{g_W}{\sqrt{2} \cos \theta_W} e^{i\phi} [(E - |\mathbf{p}|)g_L + (E + |\mathbf{p}|)g_R] \frac{1 + \cos \theta}{2} \delta^{ij} \\
\mathcal{M}^{(1)}(b^\uparrow \bar{b}^\uparrow \rightarrow \tilde{g}^\uparrow \tilde{g}^\uparrow) &= -A^{(1)} e^{-i\phi} (B_{+-} S_{\tilde{b}} - B_{-+} C_{\tilde{b}})(B_{+-} S_{\tilde{b}} - B_{-+} C_{\tilde{b}}) \frac{1 + \cos \theta}{2} \\
\mathcal{M}^{(2)}(b^\uparrow \bar{b}^\uparrow \rightarrow \tilde{g}^\uparrow \tilde{g}^\uparrow) &= A^{(2)} e^{-i\phi} (B_{--} S_{\tilde{b}} - B_{++} C_{\tilde{b}})(B_{--} S_{\tilde{b}} - B_{++} C_{\tilde{b}}) \frac{1 + \cos \theta}{2}
\end{aligned}$$

$$\begin{aligned}
\mathcal{M}(Z^\uparrow \rightarrow b^\downarrow \bar{b}^\downarrow) &= \frac{g_W}{\sqrt{2} \cos \theta_W} e^{i\phi} [(E + |\mathbf{p}|)g_L + (E - |\mathbf{p}|)g_R] \frac{1 - \cos \theta}{2} \delta^{ij} \\
\mathcal{M}^{(1)}(b^\downarrow \bar{b}^\downarrow \rightarrow \tilde{g}^\uparrow \tilde{g}^\uparrow) &= A^{(1)} e^{-i\phi} (B_{++} S_{\tilde{b}} - B_{--} C_{\tilde{b}}) (B_{++} S_{\tilde{b}} - B_{--} C_{\tilde{b}}) \frac{1 - \cos \theta}{2} \\
\mathcal{M}^{(2)}(b^\downarrow \bar{b}^\downarrow \rightarrow \tilde{g}^\uparrow \tilde{g}^\uparrow) &= -A^{(2)} e^{-i\phi} (B_{-+} S_{\tilde{b}} - B_{+-} C_{\tilde{b}}) (B_{-+} S_{\tilde{b}} - B_{+-} C_{\tilde{b}}) \frac{1 - \cos \theta}{2} \\
\mathcal{M}(Z^\uparrow \rightarrow b^\uparrow \bar{b}^\downarrow) &= -\frac{g_W m_b}{\sqrt{2} \cos \theta_W} (g_L + g_R) \frac{\sin \theta}{2} \delta^{ij} \\
\mathcal{M}^{(1)}(b^\uparrow \bar{b}^\downarrow \rightarrow \tilde{g}^\uparrow \tilde{g}^\uparrow) &= -A^{(1)} (B_{+-} S_{\tilde{b}} - B_{-+} C_{\tilde{b}}) (B_{++} S_{\tilde{b}} - B_{--} C_{\tilde{b}}) \frac{\sin \theta}{2} \\
\mathcal{M}^{(2)}(b^\uparrow \bar{b}^\downarrow \rightarrow \tilde{g}^\uparrow \tilde{g}^\uparrow) &= A^{(2)} (B_{--} S_{\tilde{b}} - B_{++} C_{\tilde{b}}) (B_{-+} S_{\tilde{b}} - B_{+-} C_{\tilde{b}}) \frac{\sin \theta}{2} \\
\mathcal{M}(Z^\uparrow \rightarrow b^\downarrow \bar{b}^\uparrow) &= \frac{g_W m_b}{\sqrt{2} \cos \theta_W} e^{2i\phi} (g_L + g_R) \frac{\sin \theta}{2} \delta^{ij} \\
\mathcal{M}^{(1)}(b^\downarrow \bar{b}^\uparrow \rightarrow \tilde{g}^\uparrow \tilde{g}^\uparrow) &= A^{(1)} e^{-2i\phi} (B_{++} S_{\tilde{b}} - B_{--} C_{\tilde{b}}) (B_{+-} S_{\tilde{b}} - B_{-+} C_{\tilde{b}}) \frac{\sin \theta}{2} \\
\mathcal{M}^{(2)}(b^\downarrow \bar{b}^\uparrow \rightarrow \tilde{g}^\uparrow \tilde{g}^\uparrow) &= -A^{(2)} e^{-2i\phi} (B_{-+} S_{\tilde{b}} - B_{+-} C_{\tilde{b}}) (B_{--} S_{\tilde{b}} - B_{++} C_{\tilde{b}}) \frac{\sin \theta}{2}
\end{aligned}$$

$\mathcal{M}$  matrix elements for  $Z^\uparrow \rightarrow \tilde{b}\tilde{b}^* \rightarrow \tilde{g}^\uparrow \tilde{g}^\uparrow$ :

$$\begin{aligned}
\mathcal{M}(Z^\uparrow \rightarrow \tilde{b}\tilde{b}^*) &= \frac{g_W}{\sqrt{2} \cos \theta_W} e^{i\phi} |\tilde{\mathbf{p}}| [g_L S_{\tilde{b}}^2 + g_R C_{\tilde{b}}^2] \sin \theta \\
\mathcal{M}^{(1)}(\tilde{b}\tilde{b}^* \rightarrow \tilde{g}^\uparrow \tilde{g}^\uparrow) &= \tilde{A}^{(1)} e^{-i\phi} |\tilde{\mathbf{p}}| (\tilde{B}_{--} S_{\tilde{b}}^2 + \tilde{B}_{++} C_{\tilde{b}}^2) \sin \theta \\
\mathcal{M}^{(2)}(\tilde{b}\tilde{b}^* \rightarrow \tilde{g}^\uparrow \tilde{g}^\uparrow) &= -\tilde{A}^{(2)} e^{-i\phi} |\tilde{\mathbf{p}}| (\tilde{B}_{++} S_{\tilde{b}}^2 + \tilde{B}_{--} C_{\tilde{b}}^2) \sin \theta
\end{aligned}$$

## References

- [1] E. L. Berger, B. W. Harris, D. E. Kaplan, Z. Sullivan, T. M. Tait and C. E. Wagner, Phys. Rev. Lett. **86**, 4231 (2001) [arXiv:hep-ph/0012001].
- [2] G. C. Cho, Phys. Rev. Lett. **89**, 091801 (2002) [arXiv:hep-ph/0204348].
- [3] E. L. Berger and L. Clavelli, Phys. Lett. B **512**, 115 (2001) [arXiv:hep-ph/0105147].
- [4] L. J. Clavelli and L. R. Surguladze, to O(alpha(s)\*\*3),” Phys. Rev. Lett. **78**, 1632 (1997) [arXiv:hep-ph/9610493].
- [5] J. j. Cao, Z. h. Xiong and J. M. Yang, Phys. Rev. Lett. **88**, 111802 (2002) [arXiv:hep-ph/0111144].
- [6] L. Clavelli, Phys. Rev. D **46**, 2112 (1992).
- [7] C. W. Chiang, Z. Luo and J. L. Rosner, arXiv:hep-ph/0207235, to be published in Physics Review D.

- [8] S. Berge and M. Klasen, Phys. Rev. D **66**, 115014 (2002) [arXiv:hep-ph/0208212].
- [9] P. Nelson and P. Osland, Phys. Lett. B **115**, 407 (1982).
- [10] B. Kileng and P. Osland, arXiv:hep-ph/9411248, Contributed to 9th International Workshop on High Energy Physics and Quantum Field Theory (NPI MSU 94), Moscow, Russia, 16–22 Sept. 1994.
- [11] I. Terekhov and L. Clavelli, Phys. Lett. B **385**, 139 (1996) [arXiv:hep-ph/9603390].
- [12] G. L. Kane and W. B. Rolnick, Nucl. Phys. B **217**, 117 (1983);
- [13] A. Djouadi and M. Drees, Phys. Rev. D **51**, 4997 (1995) [arXiv:hep-ph/9411314].
- [14] L. M. Sehgal, “Anti-Lepton And  $K(L) \rightarrow Lepton\ Anti-Lepton$ ,” Phys. Rev. **183**, 1511 (1969) [Erratum-ibid. D **4**, 1582 (1971)].
- [15] M. K. Gaillard and B. W. Lee, Phys. Rev. D **10**, 897 (1974).
- [16] M. E. Peskin and D. V. Schroeder, An Introduction to Quantum Field Theory, Perseus Books Publishing, L.L.C., 1995.
- [17] H. E. Haber and G. L. Kane, Phys. Rept. **117**, 75 (1985).
- [18] J. Erler and P. Langacker, mini-review on electroweak model and constraints on new physics in Particle Data Group, K. Hagiwara *et al.*, *Review of Particle Physics*, Phys. Rev. D **66**, 010001-98 (2002).
- [19] K. Cheung and W. Y. Keung, Phys. Rev. Lett. **89**, 221801 (2002) [arXiv:hep-ph/0205345].
- [20] R. Malhotra and D. A. Dicus, arXiv:hep-ph/0301070.
- [21] K. Cheung and W. Y. Keung, Phys. Rev. D **67**, 015005 (2003) [arXiv:hep-ph/0207219].
- [22] S. Baek, Phys. Lett. B **541**, 161 (2002) [arXiv:hep-ph/0205013].